VOL. 7, NO. 7, JULY 2012 ISSN 1819-6608
ARPN Journal of Engineering and Applied Sciences


www.arpnjournals.com

THE INFLUENCE OF Bi_2O_3 AND Sb_2O_3 DOPING ON THE MICROSTRUCTURE AND ELECTRICAL PROPERTIES OF SINTERED ZINC OXIDE

A. Yaya[1, 2] and D. Dodoo-Arhin[1, 3]
[1]Department of Materials Science and Engineering, University of Ghana, Ghana
[2]Institute des Matériaux Jean Rouxel (IMN), Université de Nantes, CNRS UMR, Nantes, France
[3]Department of Physics, Institute of Applied Materials, University of Pretoria, Pretoria 0002, RSA
E-Mail: dodooa@ing.unitn.it

ABSTRACT

The influence of Bi_2O_3 and Sb_2O_3 doping on the microstructure and electrical characteristics of Zinc Oxide based varistor has been investigated. The as-sintered ceramic varistors with different compositions have been characterized via laboratory X-ray diffraction (XRD), scanning electron microscopy (SEM), energy dispersive spectroscopy (EDS) and electrical measurements. Bismuth oxide doping resulted in liquid phase sintering, rapid densification, grain growth and electrical varistor precipitating to a spinel phase and thereby inhibiting grain growth. Electrical property measurements indicate varistor behaviour for both cases of doping.

Keywords: Bi_2O_3, Zinc oxide, Sb_2O_3, sintering, x-ray diffraction, SEM.

1. INTRODUCTION

Zinc oxide, a wide band gap semiconductor with a relatively large exciton binding energy (60 meV) and considered a highly efficient photon emitter, has in recent times received extensive attention in the scientific community as a candidate material for opto-electronic devices such as UV laser diodes and UV light emitting diodes, and as varistors to protect against any unforeseen voltage fluctuations (Zeng D. W., *et al*., 2004).

Zinc oxide with a wurtzite structure is an n-type semiconductor material with both good electrical and optical properties. This is due to deviation from stoichiometry with the existence of intrinsic defects such as oxygen vacancies and zinc interstitials (Onreabroy W., *et al*., 2005).

Due to this instability in ZnO which limits its application in some fields, doping with other substances has in most cases been adopted to improve its properties for technological purposes.

ZnO based varistors are formed by sintering a mixture of ZnO powders with small quantities of other oxides, such as those of bismuth, manganese, antimony, cobalt, chromium, etc., at a relatively high temperature. Zinc oxide varistors are ceramic semiconductors with extremely high nonlinear current-voltage behaviour and hence, are used to protect circuits against voltage surges.

Microstructural studies show that, the bismuth-rich phase can mostly be found at intergranular layers leading to the nonlinear current-voltage characteristics (Eda K, 1978; H. Cerva and W. Russwurm, 1988). These properties are considered to originate at the grain boundaries.

Research has also shown that, the non-ohmic properties occur at the intergranular layer and appear with the double Schottky barriers (DSB) (D.R. Clarke, 1999).

The high non-linear coefficient and high stability of the DSB in varistors can be improved by the addition of other oxide such as bismuth oxide (H. Cerva and W. Russwurm, 1988; J P Gambino *et al*., 1989; M. Elfwing, *et al*., 2000; L. Madler *et al*., 2002; J H. Choi *et al*., 2001), antimony oxide, which slows the grain growth processes. CoO, NiO, and MnO improves nonlinearity, whiles Al_2O_3 increases the electrical conductivity of the zinc oxide grains (C Leach, 2005; K. Mukae, *et al*., 1977; M. Matsuoka, In: Levinson LM, (ed.)., 1981.; E.M. El-Meliegy *et al*., 2004).

In this present work, we investigate the influence of Bismuth and Antimony oxides addition on the microstructure and electrical behaviour of Zinc oxide based varistors.

2. EXPERIMENTAL

2.1 Materials and specimens

Three precursor oxide powder samples were prepared by mixing specific (weight %) compositions of ZnO, Bi_2O_3 and Sb_2O_3: pure ZnO [Z composition], (99%) ZnO + (1%) Bi_2O_3 [ZB composition], and (98%) ZnO + (1%) Bi_2O_3 + (1%) Sb_2O_3 [ZBS composition] were prepared.

The powders were then mixed with 2% polyvinyl alcohol (PVA) to form a paste and compacted into disc shaped pellets (1.5g each), using a 100MPa uniaxial press. The green compacts were then sintered at 800ºC and 1050ºC for 60 minutes. The percentage densifications before sintering and after sintering were also calculated as well as their weight loses (Table-1).

Selected samples with higher densifications were embedded into a polymer (epoxy) resin and then successively polished using different size of abrasives and diamond paste grits.

The polished samples were chemically etched in a solution of NaOH for about 10mins and then washed carefully with copious amount of deionized water ($<1.8\mu Scm^{-1}$). The finished samples were then oven dried at 30ºC for further characterization.

Table-1. Average values of the percentage densification, grain size and percentage weight loss.

	T (ºC)	**t** (min)	**% ρ_o**	**% ρ**	**% P**	**% l**	**Grain size** (μm)
Z	800	60	60.2	59.5	-4.1	-1.5	0.36
	1100		59.9	85.0	-3.5	-10.7	0.76
ZB	800		61.5	84.7	-2.0	-10.6	1.87
	1100		60.7	88.2	-4.2	-12.6	6.91
ZBS	800		59.6	59.7	-1.6	-0.6	0.37
	1100		60.0	86.8	-1.3	-11.9	2.15

2.2 Characterization techniques

X-ray powder diffraction (XRD) patterns were collected on a Rigaku D/Max-(III) Bragg-Bretano diffractometer operating a copper tube at 40 kV and 30 mA. The XRD patterns were recorded in the 4-80º 2θ range with a step size of 0.05º and a counting time of 10s per step.

A Hitachi S-4100 Scanning electron microscope (SEM) equipped with an EDS analyzer was employed for the morphological, microstructure and grain size distribution characterization: prior to investigation, specimens were sputtered with a thin film of carbon to make them conductive and improve image resolution. The average grain sizes were measured from the SEM images.

The current-voltage characteristics behaviour of Bi_2O_3-ZnO varistors were measured by scanning the direct current electric field at low rate. In order to protect the varistors from fusion, the measurement were terminated when the current flowing through the varistor reached a value of 24 mA.

3. RESULTS AND DISCUSSIONS

3.1 Synthesis

In the synthesis of ZBS samples, sintering at 800ºC for 60 minutes resulted in the reduction in densification with an average densification value of 59.7%. The corresponding SEM images (Figure-5) indicate no significant variation in grains morphology from the original powder compact. This could be attributed to the formation of a pyrochlore phase ($Zn_2Bi_3Sb_3O_{14}$) as shown in equation (1) below.

$$4ZnO + 3Bi_2O_3 + 3Sb_2O_3 \xrightarrow{800^\circ C} 2Zn_2Bi_3Sb_3O_{14} + 4O_2 \quad (1)$$

Due to the formation of this phase, the energy barrier required for effective densification to take place in the sample is very high and therefore resulting in a lower densification value (Figure-5b).

As the sintering temperature is increased, the pyrochlore phase precipitated a second solid phase called the spinel phase which inhibits grain growth in the sample, by pinning the grain boundaries. The formation of the spinel is as shown in the equation below:

$$2Zn_2Bi_3Sb_3O_{14} + 17ZnO \xrightarrow{>800^\circ C} 3Zn_7Sb_2O_{12} + 3Bi_2O_3 \quad (2)$$

The spinel phase ensured that pores were not trapped inside the grains and this increased the final densification of the sample. The presence of the Bismuth rich liquid phase enhanced initial densification and later, fast grain growth of the samples.

As sintering temperature increases, thus, from 800ºc to 1100ºC, a significant change in the grain size for each of the compositions is observed. Similar thing can be said about the rate of densification, when there is an increase in temperature from 800ºC to 1100ºC. It can be argued that, during the sintering processes, temperature control is an important parameter in achieving grain growth and density compacts. This was evident in the average values calculated for each composition at these two temperatures (Table-1).

This trend was observed based on the fact that, the driving force for sintering is reduction in surface energy which results in densification and a reduction in surface area which also result in Grain growth. This process is faster when the temperature is higher.

In the case of pure ZnO, the green compacts were observed to have similar grains but differ in morphology as seen in the SEM images in Figure-3. After sintering at 800ºC for 60 mins, an intermediate densification stage was observed (Figure-1) in the Z composition characterized by neck formation and the presence of interconnected pores. The rate of densification also increased when the temperature was increased to 1100ºC. The microstructure in Figure-3(b) shows the formation of neck growth which occurs between particles of different sizes and continues until the neck is no longer in the region of minimum cross-sectional area. The densification becomes much intense at 1100°C as in Figure-3(c); a further much densified microstructure would result if the temperature were to be raised further.

The SEM images of ZB composition sintered at different temperatures are shown in Figure-4 where there is evidence of microstructure evolution of the ZnO, due to the addition of bismuth.

The presence of Bismuth creates a liquid phase that allows mass transfer between the grains, (see Figure-4a) leading to a more densified microstructure as the temperature is increased (Figure-4b). This is evident by the fact that, the liquid phase created by bismuth results in

higher densification with ZB composition having the highest value of 88.2% among all the three compositions (Table-1).

ZnO-Bi_2O_3 phase diagram indicates that, at a temperature above 750ºC, there is a co-existence of the ZnO and a liquid phase, which also agrees with our SEM image given in Figure-4 for the ZB composition. EDS analysis (Figure-6a) also confirms the presence of Bismuth and Zinc rich liquid phase.

3.2 X-ray diffraction and Scanning Electron Microscopy analysis

The XRD patterns of ZBS composition (Figure-2) sintered at 800°C and 1100°C indicates the occurrence of phase transitions. For the samples sintered at 800°C (Figure-2a), only two phases (ZnO and pyrochlore phases), were observed. However, for the samples sintered at 1100°C (Figure-2b), appearance of three different phases (ZnO, pyrochlore and spinel phases) resulted. The relatively shaped peak is an indication of the crystal growth which are narrower for 1100ºC sintered samples. The energy dispersive spectroscopy (EDS) pattern (Figure-6) taken from the sample indicate the presence of the Antimony, Bismuth and Zinc.

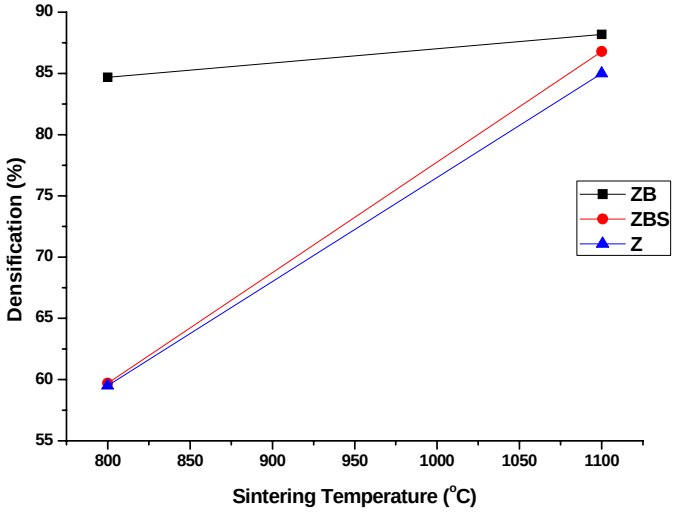

(a)

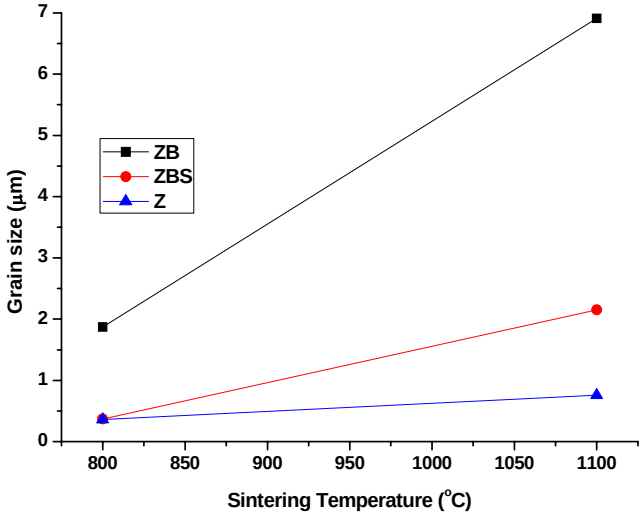

(b)

Figure-1. Graph of (a) percentage densification and (b) grain growth vs. sintering temperature.

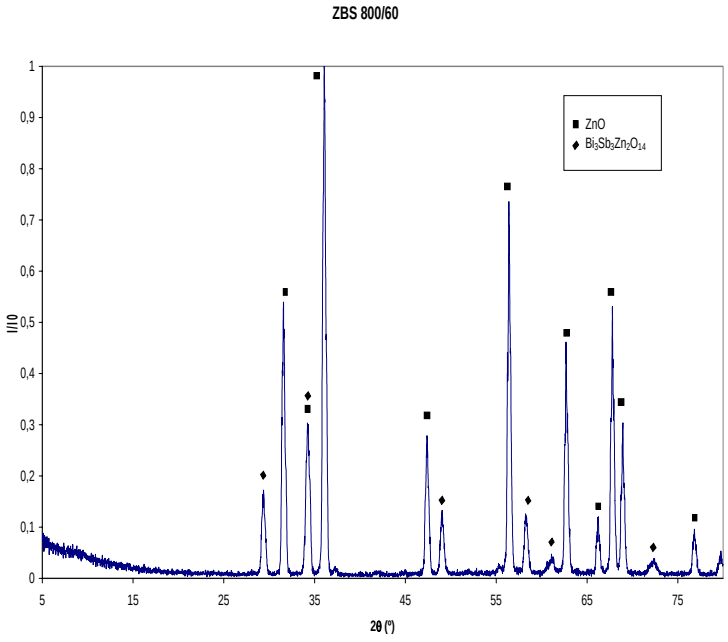

(a)

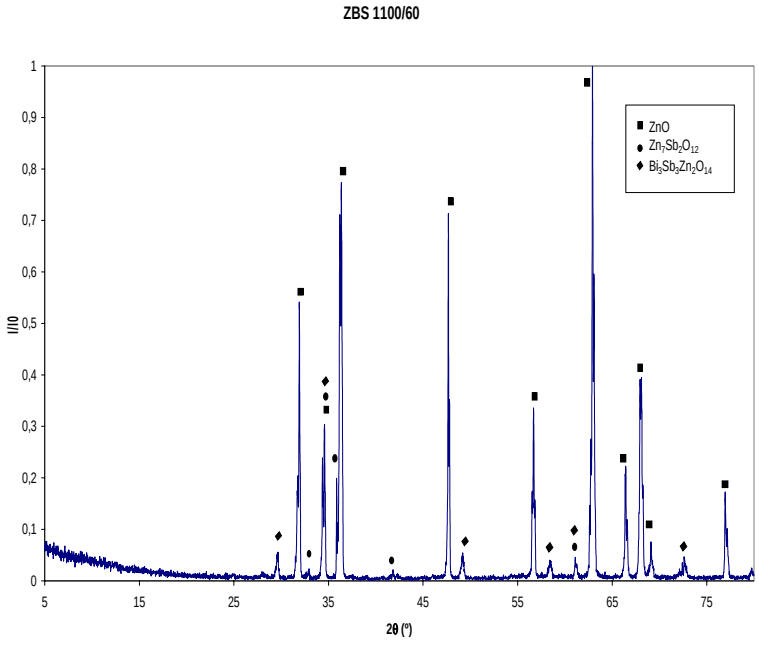

(b)

Figure-2. XRD pattern of ZBS composition with different sintering temperature of (a) 800°C and (b) 1100°C. ■-ZnO, ●- $Zn_7Sb_2O_{12}$, ♦ - $Bi_3Sb_3Zn_2O_{14}$

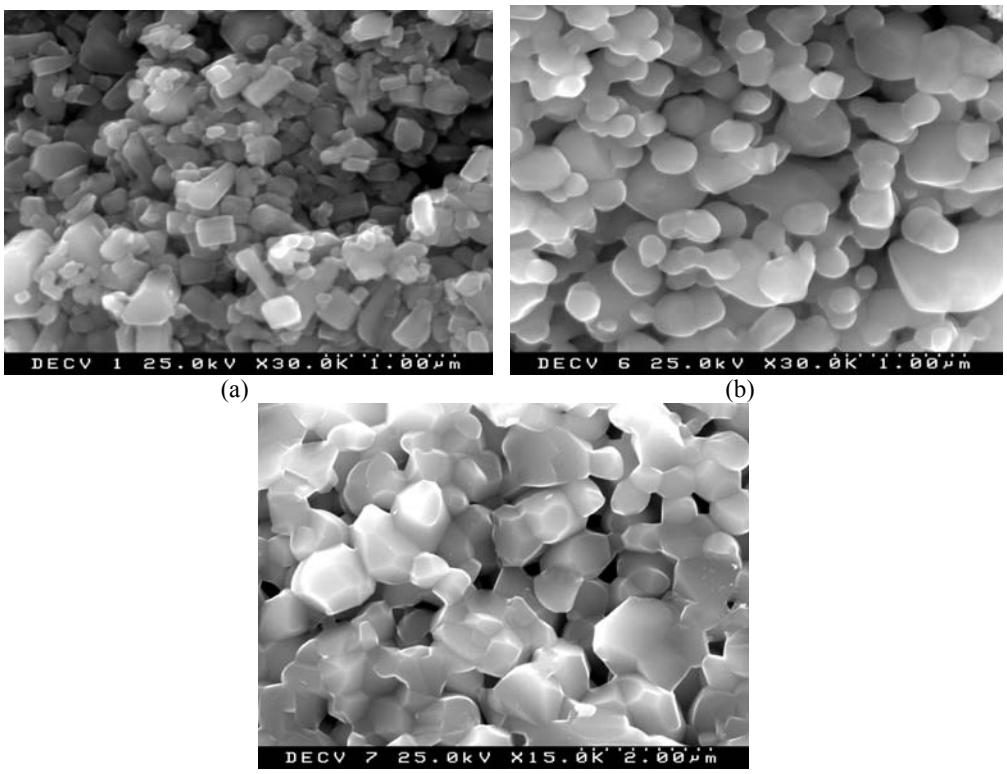

(a) (b)

(c)

Figure-3. SEM images of Z composition showing microstructural effects for (a) green compact and sintered phases for 60mins with (b) 800°C and (c) 1100°C

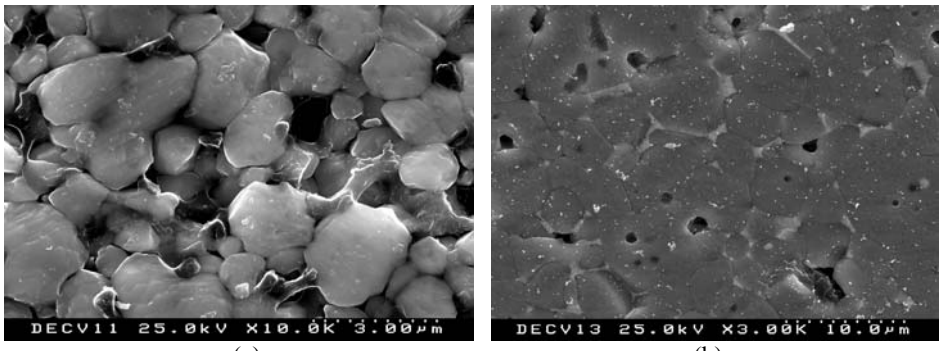

(a) (b)

Figure-4. SEM images showing microstructures of ZB at different sintering temperatures for 60 mins (a) 800°C and (b) 1100°C.

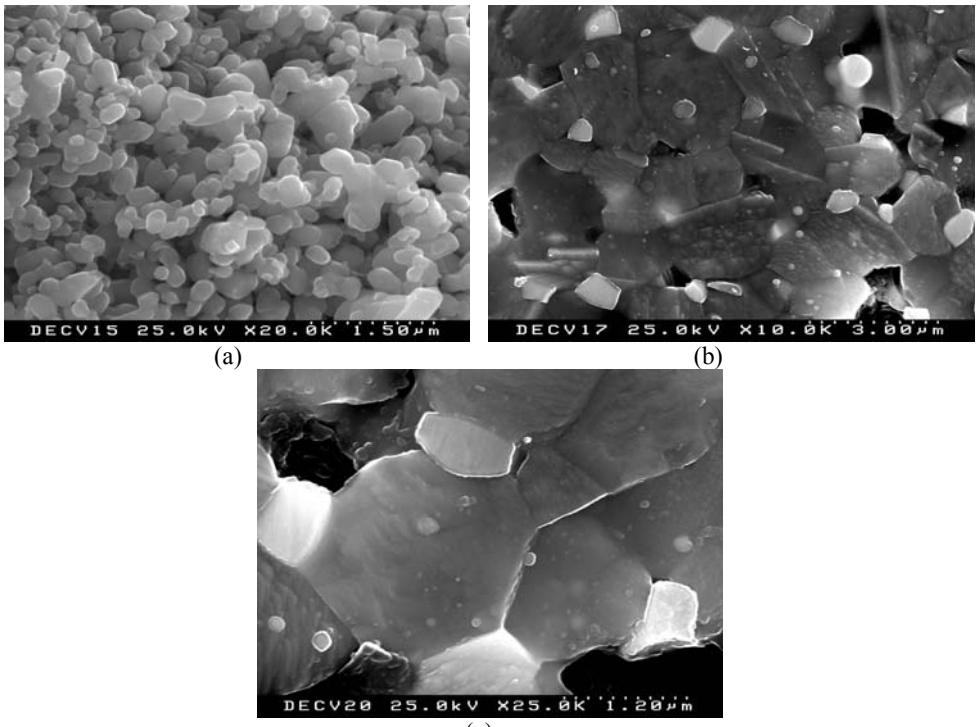

(a) (b)

(c)

Figure-5. SEM images showing the microstructures of ZBS sintered for 60 mins at temperatures of (a) 800°C, (b) 1100°C and (c) spinel phase at 1100°C.

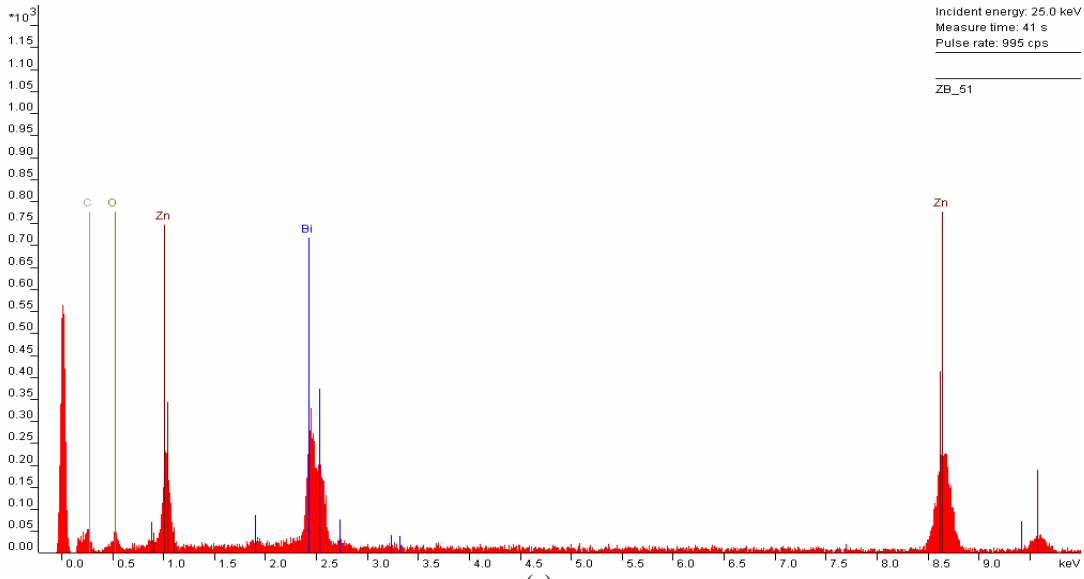

(a)

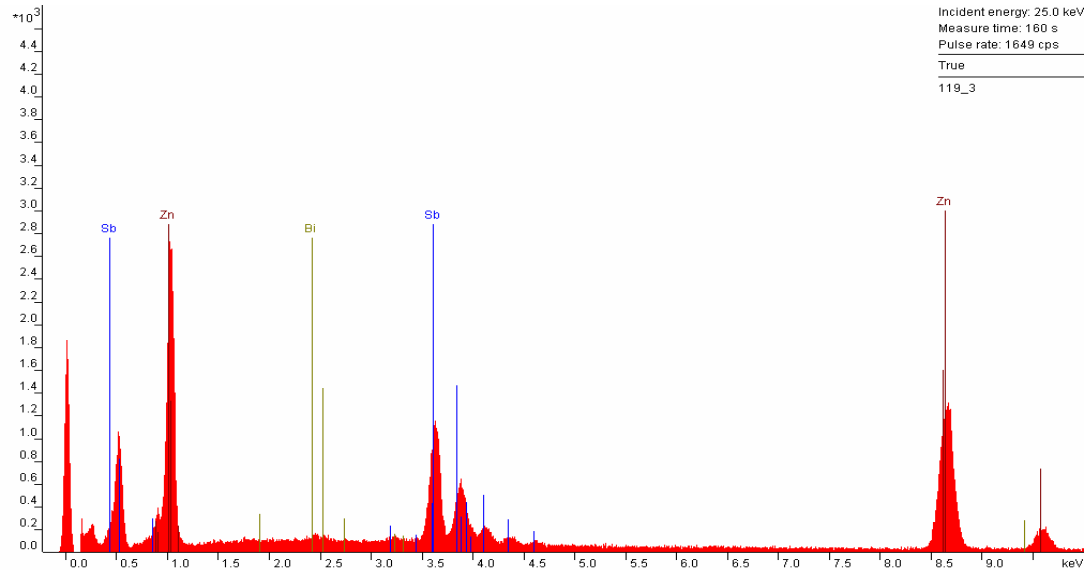

(b)

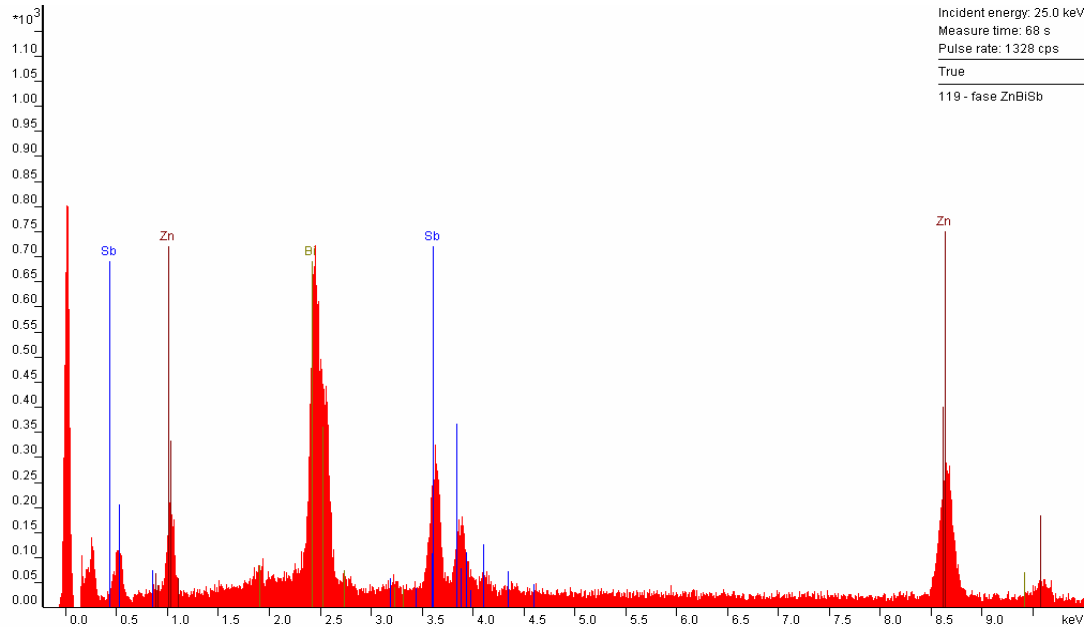

(c)

Figure-6. EDS of (a) liquid phase (sample ZB 800/60), (b) spinel phase (sample ZBS 1100/60) and (c) liquid phase around the spinel phase (sample ZBS 1100/60).

3.3 Electrical behaviour

In Figure-7, a plot of the electric field against current density for the Z composition shows a linear relationship due to its ohmic behaviour whiles for the ZB composition, a non-ohmic behaviour is observed leading to a non-linear curve.

This phenomenon is due to the fact that the addition of bismuth to ZnO produced a separated layer of bismuth phases at grain boundaries whose resistance exhibits a pronounced dependence on voltage. The junction between each grain and its neighbour forms a diode junction which allows current to flow in only one direction. When a small or moderate voltage was applied across the electrodes, only a tiny current flowed, and this is attributed to a reverse leakage through the diode junction. When a large voltage is applied, the diode junction breaks-down due to the Avalanche effect and large current flows. The result is a highly nonlinear I-V characteristic in which the metal oxide varistor has a high resistance at low voltages and a low resistance at high voltages.

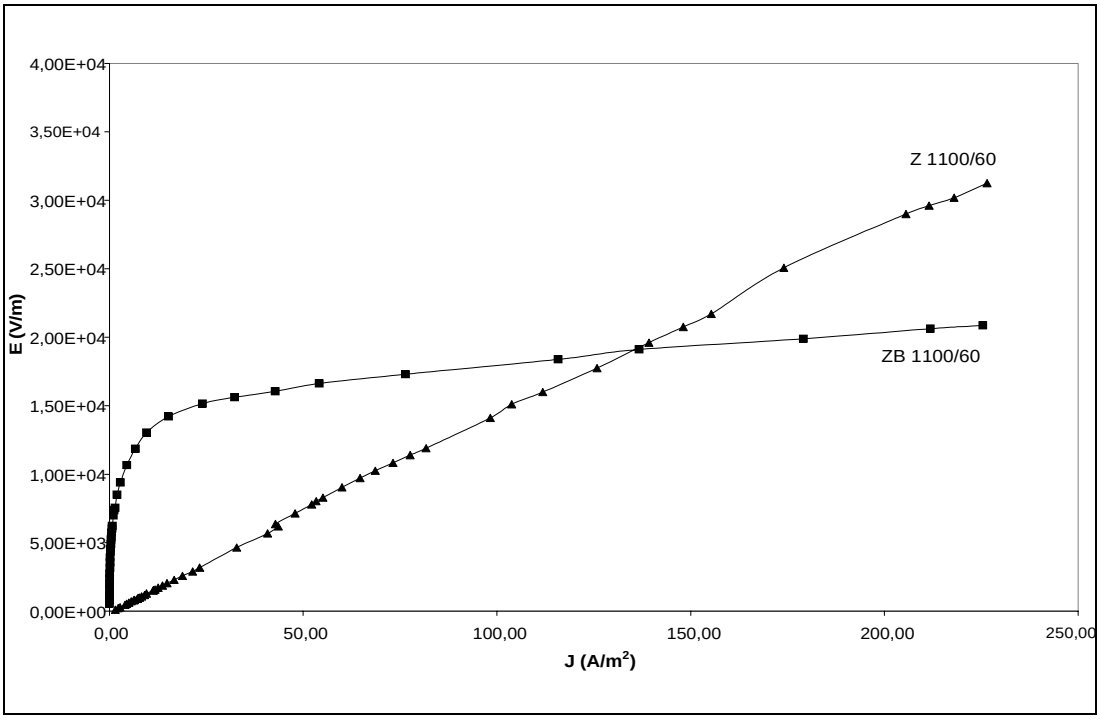

Figure-7. A plot showing ohmic and non-ohmic behaviour in Z and ZB, respectively.

4. CONCLUSIONS

The influence of the addition of Bi_2O_3 and Sb_2O_3 on the microstructure of ZnO based varistors has been studied. Sintering at high temperatures facilitates grain growth. Furthermore, when there is a liquid phase in-between the sintering time, faster densification is promoted, by allowing mass transfer of constituents. The highest percentage densification and grain growth was observed in the ZB composition. The addition of Bi_2O_3 facilitated the sintering process by forming the Bismuth rich liquid phase at the grain boundary. Addition of Sb_2O_3 to the other powder compositions made possible the formation of the pyrochlore phase which later precipitated the second solid phase (spinel) thereby reducing the grain growth rate by pinning the grain boundary.

ACKNOWLEDGEMENTS

The authors wish to acknowledge the University of Aveiro (Portugal) ceramics laboratory for use of facilities and University of Ghana for support.

REFERENCES

Cerva H. and Russwurm W. 1988. Microstructure and crystal structure of bismuth oxide phase in zinc oxide varistor ceramics. J Am Ceram Soc. 71(7): 522-30.

Choi J H., Hwang N M. and Kim D Y. 2001. Pore-Boundary Separation Behaviour during Sintering of Pure and Bi_2O_3-Doped ZnO Ceramics. J Am Ceram Soc. 84(6): 1398- 400.

Clarke D.R. 1999.Varistor ceramics. Journal of American Chemical Society. 82, 3: 485-502.

Eda K. 1978. Conduction mechanism of non-ohmic zinc oxide ceramics. J. Appl. Phys. 49(5): 2964-2972.

Elfwing M., Osterlund R. and Olsson E. 2000. Differences in wetting characteristics of Bi_2O_3 polymorphs in ZnO varistor materials. J. Am Ceram Soc. 83(9): 2311- 2314.

El-Meliegy E.M., Saleh H.I. and Selim M. 2004. Sintering and characterization of bismuth-oxide-containing zinc oxide varistors. Materials Characterization. 52: 371- 378.

Gambino J P, Kingery W D, Pike G E, Levinson L M, and Philipp H R. 1989. Effect of heat treatments on the wetting behaviour of bismuth-rich intergranular phases in bismuth- and cobalt doped zinc oxide varistors. J. Am Ceram Soc. 72(4): 642-645.

Leach C. 2005. Grain Boundary Structures in Zinc oxide Varistors. Acta Materialia. 53: 237-245.

Madler L. and Pratsinis S E. 2002. Bismuth oxide nanoparticles by flame spray pyrolysis. J. Am Ceram Soc. 85(7): 1713-1718.

Matsuoka M.1981. Progress in research and development of zinc varistors. In: Levinson LM, (ed.). Grain boundary phenomena in electronic ceramics. Advances in ceramics, 1. American Ceramic Society. pp. 290-308.

Mukae K., Tsuda K. and Nagasawa I. 1977. Non-ohmic properties of zinc oxide–rare earth metal oxide–cobalt oxide (Co_3O_4) ceramics, Japan. J. Appl Phys. 16(8): 1361-1368.

Onreabroy W., Tunkasiri T. and Sirikulrat N. 2005. Effects of Alumina Surrounding in Sintering Process on ZnO-Bi_2O_3Varistors Doped with CoO. Materials Letters. 59: 283-288.

Zeng D. W., Xie C.S., Zhu B. L., Jiang R., Chen X., Song W.L, Wang J.B. and Shi J. 2004. Controlled growth of ZnO nanomaterials via doping Sb. Journal of Crystal Growth. 266: 511.